

# Nonlinear linear dynamics and numerical analysis of a sloshing tank

Mauricio Aparecido Ribeiro<sup>1</sup>, Jose Manoel Balthazar<sup>1,2</sup>, Maria Aline Gonçalves<sup>3</sup>, Angelo Marcelo Tusset<sup>1</sup>, Raphaela C. Machado<sup>4</sup>

<sup>1</sup>*Dept. of Electrical, Universidade Tecnológica Federal do Paraná  
Rua Doutor Washington Subtil Chueire, 330 - Jardim Carvalho 84017-220 Ponta Grossa, Paraná, Brazil  
mau.ap.ribeiro@gmail.com*

<sup>2</sup>*Mechanical Faculty, Universidade De São Paulo- UNESP  
Av. Eng. Luiz Edmundo C. Coube 14-01 - Vargem Limpa - Bauru - SP/SP - CEP 17033-360  
jmbaltha@gmail.com*

<sup>3</sup>*Dept. of Electrical, Centro Universitário Internacional  
R. Voluntários da Pátria, 290 - Centro, Curitiba - PR, 80020-000, Paraná, Brazil  
a.m.tusset@gmail.com*

<sup>4</sup>*Faculdade de Engenharia de Guaratinguetá, Universidade de São Paulo- UNESP  
Avenida Doutor Ariberto Pereira da Cunha, Portal das Colinas, 12516410, São Paulo, Brazil*

**Abstract.** Sloshing motion in liquids refers to the phenomenon of oscillation or agitation that occurs when a liquid is subjected to movement or disturbance. This can happen in containers, tanks, ships, or any other object that contains liquid and is subject to movement, such as acceleration, deceleration, turning or tilting. These oscillations can be caused by several factors, such as sudden changes in speed, changes in the direction of movement, winds, waves, or even internal movements of the liquid due to its own inertia. Sloshing can have significant effects in different contexts, such as naval engineering, liquid cargo transportation, storage tank projects, among others. Therefore, the study of sloshing is important to ensure the safety and stability of structures that contain moving liquids, as the forces resulting from these oscillations can affect structural integrity and even lead to accidents if they are not properly considered and controlled. Mathematical models and computer simulations are often used to predict and mitigate the effects of sloshing in different applications. Thus, this work investigates a mathematical model that describes a tank coupled to an electric motor, and therefore we determine the parameter space of the Lyapunov Exponent, bifurcation diagrams and phase maps. These numerical analyses are important to determine the range of parameters that diagnose chaos in the system

**Keywords:** Nonlinear Linear Dynamics, Chaos, Numerical analysis, Sloshing tank, Applications to engineering

## 1 Introduction

In fluid dynamics, liquid slosh refers to the movement of liquid within another object. Strictly speaking, the liquid must have a free surface to constitute a slosh dynamics problem, where the dynamics of the liquid can interact with the container to significantly alter the dynamics of the system. Analyzes of nonlinear dynamic behavior are extremely important to determine the parameters that may or may not occur in chaos phenomena in vibrations inside the tank that transports the liquid. Classic examples of this transport are the fuel tanks on aircraft such as planes and cargo-carrying rockets [1-12].

Authors such as [14-18] analyze the behavior of oscillation dynamics through CFD that compare computational and experimental results to investigate the relative speed of the fluid interface to confirm mathematical models that are proposed.

However, CFD analyzes can have a high computational cost to obtain results, thus analyzes with mechanical systems using mathematical modeling with the Lagrange formalism considering the system's energies. In this way, considering such formalism supports the understanding of a more global scale of the vibrations that occur in the mechanism and has a higher computational cost if we compare the CFD.

One issue highlighted is the liquid propellant fuel tank, as concerns in the design of liquid propellant rockets include movement of the center of mass, vehicle attitude, and lateral bending of the vehicle structure. Shaking technology developed for space applications is not applicable to tank trucks because emphasis has been placed on frequencies and total forces related to control system requirements and therefore the effects of local impact pressure peak on structural requirements have not been studied to any extent. Furthermore, the excitation amplitudes considered in space applications are too small for road vehicle simulation. In tank trucks, the liquid-free surface can undergo large excursions even for very small movements of the container. This is an undesirable characteristic, which can considerably compromise the stability and handling quality of the vehicle. This problem is common in fuel or cargo tanks of motor vehicles, railway tank cars, fuel tanks of large ships and tankers. The study of the dynamics of liquid movement within a moving vehicle involves different types of modeling and analysis [15-24].

Therefore, our manuscript investigates the nonlinear dynamic behavior in numerical form, the system consisting of a tank containing a liquid coupled to a non-ideal engine. To do this, we analyze the nonlinear dynamic behavior with the Lyapunov exponent, which describes the divergence of phase space trajectories. This analysis allows investigating and diagnosing the parameter space and defining possible regions in which the system presents chaotic or periodic behavior.

## 2 Mathematical Modeling

According to [9] the movement of the liquid on the surface of the tank can have a chaotic or regular behavior. The surface of the liquid inside the tank is described by the linear combination of the sums of the vibration eigenmodes  $\eta(r, \theta, t) = \eta_n(t)\psi_n(r, \theta)$ , where the sum is performed at indices i and j, therefore:

$$\eta(r, \theta, t) = \sum_{i,j} [q_{i,j}^c(t)k_{i,j}(r)\cos(i\theta) + q_{i,j}^s(t)k_{i,j}(r)\sin(i\theta)] \quad (1)$$

Eq. (1) was obtained by applying the traditional boundary problem solution procedure using the variable separation method. This way, each index i or j has its own functions, frequency and parameters. To analyze Eq. (1), Miles in Refs. [9] proposed the sum of identical indices, so that the regular or chaotic movement is presented by Eq. (1) which is characterized by the fundamental amplitudes and the secondary vibration motors that represent an approximation of the irregularities of the free surface of the liquid. According to the authors in Ref. [9, 10] they assume that the resonant oscillations of the liquid surface are approximated by:

$$\eta \approx \eta_1 k_{nm}(r) \cos(n\theta) + \eta_2 k_{n,m}(r) \sin(n\theta) \quad (2)$$

with:

$$\eta_n(t) \propto [p_n(\tau) \cos(\sigma(t)) + q_n(\tau) \sin(\sigma(t))] \quad (3)$$

with  $n = 1, 2$ . Where  $p_n$  e  $q_n$  represent the amplitudes. However, the Lagrange equation is defined by:

$$L = \frac{1}{2} \{ I \dot{\sigma}^2 + m_0 \dot{v}^2 + \rho S [a_{mn} \dot{\eta}_m \dot{\eta}_n - (g + \ddot{v}) \eta_n \eta_n] \} \quad (4)$$

where  $S$  is the cross-sectional area of the tank,  $I$  is the moment of inertia of the electromotor shaft,  $m_0$  is the mass of the tank,  $\rho$  is the density of the fluid,  $g$  is the acceleration of gravity,  $\ddot{v}$  is the vertical acceleration of the tank, and  $a_{mn}$  are nonlinear functions of  $\eta_n$ . The angular speed of the electromotor shaft depends on the characteristics of

the electric motor and the vibration of the fluid, and this speed cannot be a prescribed value. This occurs because the power of the electromotor, which excites the vertical vibrations of the tank, is comparable to the power dissipated in the fluid in the damping process. As mentioned before, the tank is displaced in space according to  $y(t) = x_0 \cos \delta(t)$ . Placing vertical accelerations  $\ddot{v}$  em  $L$ , we obtain an expression for the angle  $\delta(t)$ ,

$$L = \frac{1}{2} \{ I \dot{\delta}^2 + m_0 x_0^2 \dot{\delta}^2 \sin^2(\delta) + \rho S [a_{mn} \dot{\eta}_m \dot{\eta}_n + [x_0 (\dot{\delta}^2 \cos(\delta) + \ddot{\delta} \sin(\delta)) - g] \eta_m \eta_n] \} \quad (5)$$

Podendo ser derivado da equação de Lagrange pelas coordenadas generalizadas do motor  $\delta$  com

$$I \ddot{\delta} = -m_0 x_0^2 \ddot{\delta}(\delta) - m_0 x_0^2 \dot{\delta}^2 \sin(\delta) \cos(\delta) + \rho S x_0 (\dot{\delta}^2 \sin(\delta) - \ddot{\delta} \cos(\delta)) \eta_n \eta_n - 2\rho S x_0 \dot{\delta} \cos(\delta) + \Psi(\dot{\delta}) - H(\delta) \quad (6)$$

The vibration of the free surface is approximated by dominant and secondary modes:

$$\eta_n = \sqrt{\frac{x_0 \omega_1^2}{g}} \lambda \left[ p_n(\tau) \cos\left(\frac{\delta}{2}\right) + q_n(\tau) \sin\left(\frac{\delta}{2}\right) \right] \quad n = 1, 2 \quad (7)$$

and for the amplitude of the secondary modes,

$$\eta_n = \frac{x_0 \omega_1^2}{g} \lambda [A_n(\tau) \cos(\delta) + B_n(\tau) \sin(\delta) + C_n(\tau)] \quad n \neq 1, 2 \quad (8)$$

Following the authors' procedure, that is, we can write an expression for the mean Lagrangian ( $L$ ), so:

$$\langle L \rangle = \frac{1}{2} I \dot{\delta}^2 + \frac{1}{4} m_0 x_0^2 \dot{\delta}^2 + \frac{1}{2} \left( \frac{x_0 \omega_1^2}{g} \right)^4 \lambda^2 \rho S \left[ \frac{1}{2} \left( \frac{dp_n}{d\tau} q_n - p_n \frac{dq_n}{d\tau} \right) + p_1 + \frac{\delta}{\omega_1^2} q_1 + \beta E + \frac{AE^2}{2} + \frac{BM^2}{2} \right] \quad (9)$$

The Hamiltonian equations, described by Eq. (9), and we obtain the system presented in Eq. (10) for the temporal evolution of the equations, where the last equation for closes the system Eq. (10) and is obtained with the characteristics of the electric motor, however:

$$\begin{aligned} \frac{dp_1}{d\tau} &= \alpha p_1 - (\beta + AE - 2)q_1 + BMp_2 \\ \frac{dq_1}{d\tau} &= -\alpha q_1 + (\beta + AE + 2)p_1 + BMq_2 \\ \frac{dp_2}{d\tau} &= -\alpha p_2 - (\beta + AE - 2)q_2 - BMp_1 \\ \frac{dq_2}{d\tau} &= -\alpha q_2 + (\beta + AE + 2)p_2 - BMq_1 \\ \frac{d\beta}{d\tau} &= N_2 - N_1\beta - \mu(p_1q_1 + p_2q_2) \end{aligned} \quad (10)$$

where  $E = \frac{1}{2}(p_1^2 + q_1^2) + \frac{1}{2}(p_2^2 + q_2^2)$  and  $M = p_1q_2 - p_2q_1$ ,  $N_1$  and  $N_2$  are depending on constants of the linear static performance curve of the motor,  $N_2$  is also a function of the natural frequency of the free surface oscillations, and  $\mu$  is a parameter in function of the natural frequency and physical characteristics of the motor which measures the offset of frequencies. A and B are constant coefficients.

In Fig. (1) show the scheme considered for moving the oscillations of the tank containing liquid coupled to a motor to cause the oscillations containing the liquid.

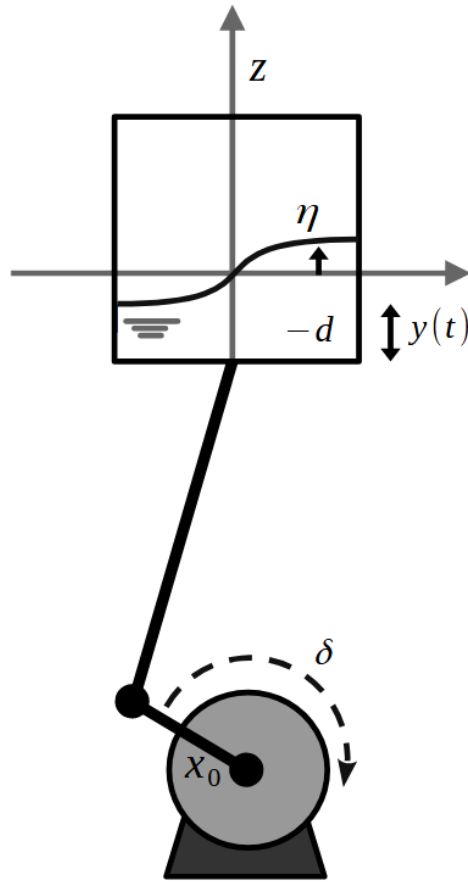


Fig. (1): Mechanical scheme, where  $\delta$  is the engine rotation,  $\eta$  is the linear combination of the sums of the vibration eigenmodes,  $y(t)$  external force that moves the tank containing the liquid,  $-d$  represents the lower part of the liquid.

### 3 Numerical Results

For numerical analyses, we used the parameters described in Tab. (1) and the following initial condition  $[0.1, 0.1, 1.0, 1.0, 0.0]$ , we used the 4th order Runge-Kutta integrator, with a total integration time of  $10^6$ [s] and considering a transient time of 40% of the total time.

Tab (1): Parameter for numerical analysis.

Parameters	Values
A	1.112
B	-1,531
$N_2$	-0.25
$\alpha$	0.8

As a first analysis, we investigated the maximum Lyapunov exponent ( $\lambda_{max}$ ), which describes the behavior of phase space trajectories. The Fig. (2)(a) shows the behavior of  $\lambda_{max} < 0$  considering  $N_1 \in [3.5, 4.0] \times \mu \in [0, 1]$ , the region in black shows the periodic behavior of the system, that is,  $\lambda_{max} > 0$  and for the colors between purple and yellow, that is,  $\lambda_{max} > 0$  the chaotic behavior of the system [12-14]. The interesting thing to be observed are the shrimp-like structures that appeared within the parameters obtained in Fig. (1). According to [15,19] shrimp-like structures are formed by the regular set of adjacent windows centered around the main pair of intersecting superstable arches. Such structures are infinite mosaics of stability domains doubly composed of one main innermost domain but all adjacent stability domains arising from two period-folding

cascades together with their corresponding chaotic domains [20, 26]. The Fig. (2)(b) shows a rough image of the shrimp-like patterns found in the parameter space determined by  $\lambda_{max}$

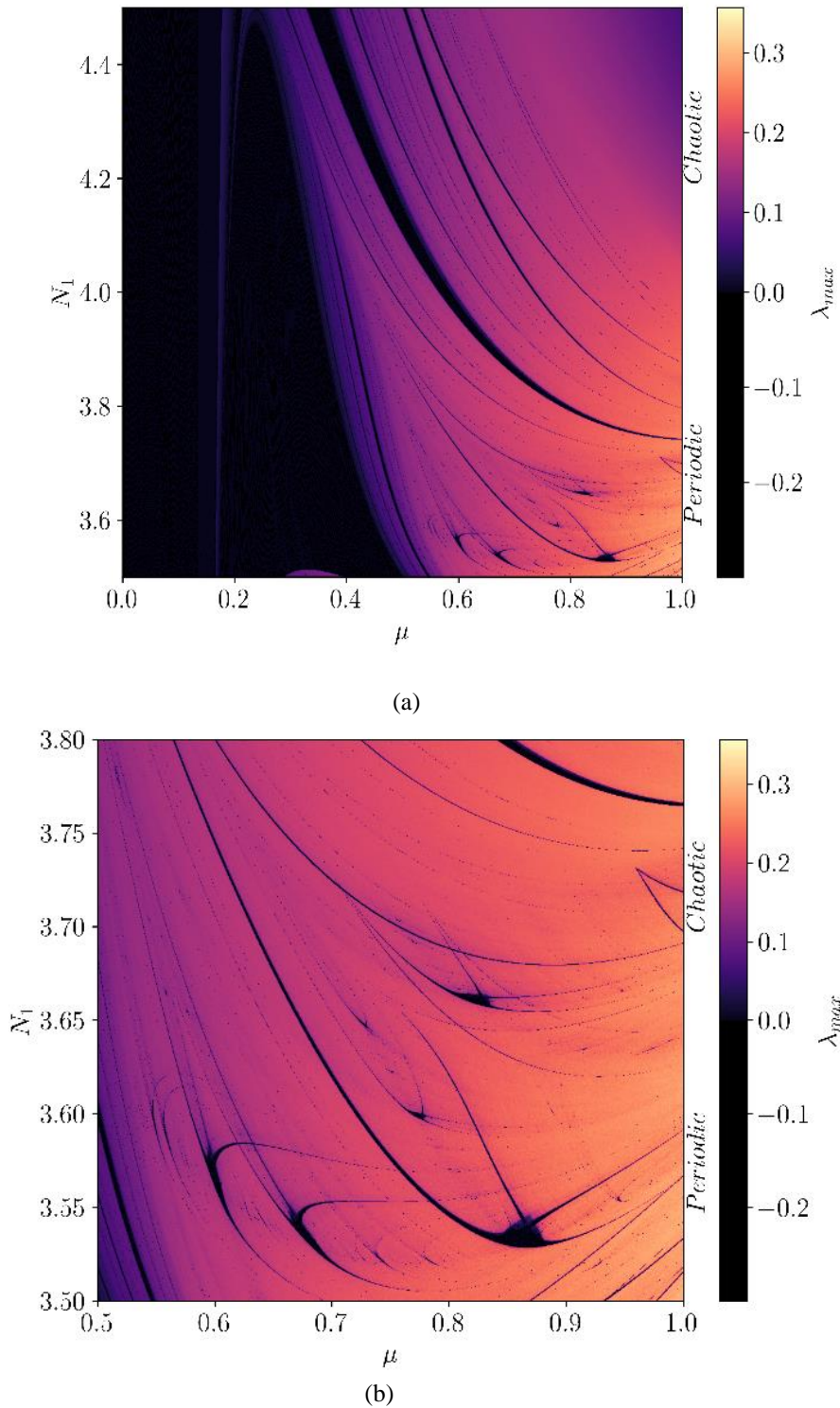


Fig (2): Maximum Lyapunov Exponent. (a)  $N_1 \in [3.5, 4.0] \times \mu \in [0,1]$  and (b)  $N_1 \in [3.5, 3.8] \times \mu \in [0.5,1]$  zoom for shrimp observation.

For a more specific analysis, we do not consider the value of  $N_1 = 3.5351$  because with the variation of  $\mu \in [0,1]$  the intersection with the shrimp-type structure and thus we can observe the behavior of the bifurcation

diagram as shown in Fig. (3)(a), to confirm the periodic windows determined by the bifurcation diagram, the corresponding intervals determined by the bifurcation diagram are described in Tab. (1)

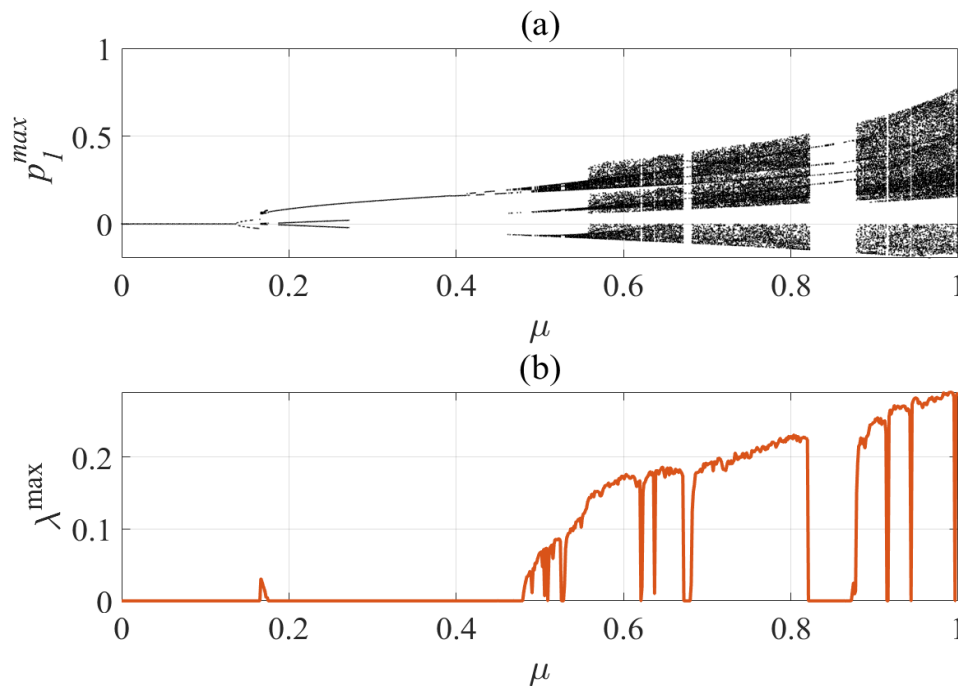
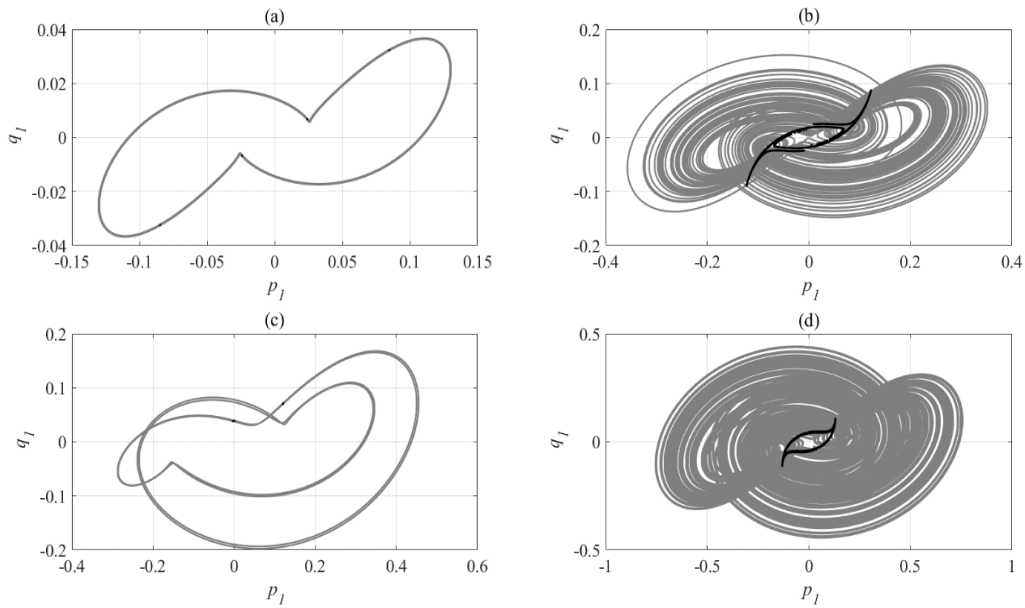


Fig. (3): (a) Diagram bifurcation for  $\mu \in [0,1]$  e  $N_1 = 3.5351$  and (b) maximum Lyapunov Exponent  $\mu \in [0,1]$  e  $N_1 = 3.5351$  .

Tab. (1): Range of  $\mu$  determined by the bifurcation diagram

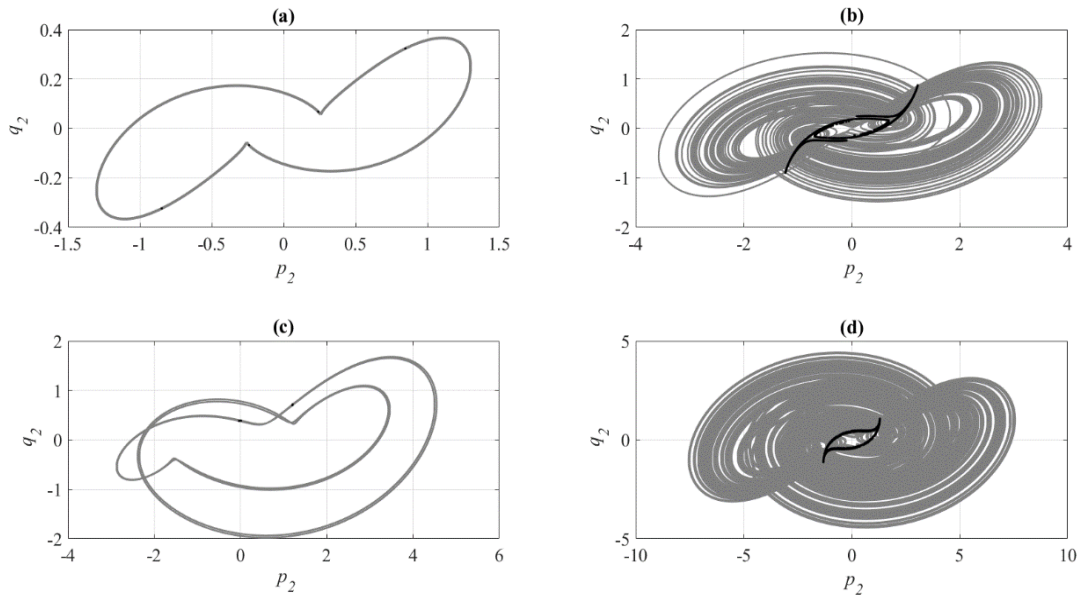
Range of $\mu$	Behavior
[0.0, 0.1600]	
[0.1700, 0.4793]	
[0.5257, 0.5282]	
[0.6208, 0.6211]	
[0.6721, 0.6792]	<i>Periodic Behavior</i>
[0.821, 0.8723]	<i>See Fig (3)(a)</i>
[0.9149, 0.9116]	
[0.9437, 0.9440]	
[0.9962, 0.9965]	

In this way, we can define the behavior of the phase maps considering the analyzes of the bifurcation diagram and the Poincaré maps. The Fig.(4)(a), Fig. (4)(b), Fig. (4)(c) and Fig. (4)(d) the gray line represents the behavior of the system's phase map defined by Eqs. (10) and black dots show the Poincaré maps.



Figs. (4): Phase maps (gray line) and Poincaré maps (black dots) for  $p_1 \times q_1$ . (a)  $\mu = 0.1476$ , (b)  $\mu = 0.605757$ , (c)  $\mu = 0.857322$  and (d)  $\mu = 0.645227$ .

The Fig. (5)(a), Fig. (5)(b), Fig. (5)(c) and Fig. (5)(d) the gray line represents the behavior of the system's phase map defined by Eqs. (10). The black dots represent the Poincaré maps.



Figs. (5): Phase maps (gray line) and Poincaré maps (black dots) for  $p_2 \times q_2$ . (a)  $\mu = 0.1476$ , (b)  $\mu = 0.605757$ , (c)  $\mu = 0.857322$  and (d)  $\mu = 0.645227$ .

## 4 Conclusions

This work analyzes nonlinear wave motion in a tank excited by a nonideal energy source. Free surface oscillations have a chaotic behavior depending on the parametric settings in the electromotor. The nonlinear dynamic analysis of the proposed system showed that the sweep of parameters  $N_1$  and  $\mu$  considering the maximum Lyapunov exponent showed the emergence of structures called shrimps. Such structures are formed by the regular set of adjacent windows centered around the main pair of intersecting super stable arches. That is, in the case of parameters  $N_1$  and  $\mu$  which are related to the electric motor and thus changing the rotation dynamics applied to the system. In this way, we observe changes in the nonlinear dynamic behavior of the liquid surface vibration as observed at the maximum Lyapunov exponent. We observe the periodic windows for  $N_1=3.5351$  and the sweep of  $\mu \in [0,1]$ , such a value of  $N_1$  with the sweep of  $\mu$  passes through the center of the shrimp structure and thus the period presented by the bifurcation diagram can be observed. structure. Through this bifurcation diagram we can determine for some values of  $\mu = 0.1476$ ,  $\mu = 0.605757$ ,  $\mu = 0.857322$  and  $\mu = 0.645227$  determine the phase maps with their respective Poincaré maps and thus observe the chaotic and periodic behavior with the change of parameter  $\mu$ . Such non-linear dynamic analyzes help to determine parameters and thus develop control projects that can suppress chaotic behavior for some orbit of interest that is periodic obtained by relevant algebraic methods, such as the harmonic balance method. Therefore, future work is a control design like SDRE that is based on the Riccati equation that could suppress the chaotic behavior of liquid surface vibrations described in the mathematical model of our manuscript for a periodic orbit.

**Acknowledgements.** The authors thank Conselho Nacional de Desenvolvimento Científico e Tecnológico (CNPq) and Fundação de Amparo à Pesquisa do Estado de São Paulo (FAPESP) for financial support.

**Authorship statement.** The authors confirm that they are solely responsible for the authorship of this work, and that all material included here as part of the present work is owned (and authored) by the authors or has permission from the owners to be included here. There is no conflict of interest.

## References

- [1] Ibrahim, R. A. (2005). *Liquid sloshing dynamics: theory and applications*. Cambridge University Press.
- [2] Ibrahim, R. A., Pilipchuk, V. N., Ikeda, T. (2001). Recent advances in liquid sloshing dynamics.
- [3] Akyildiz, H., Ünal, E. (2005). Experimental investigation of pressure distribution on a rectangular tank due to the liquid sloshing. *Ocean Engineering*, 32(11-12), 1503-1516.
- [4] Liu, D., Lin, P. (2008). A numerical study of three-dimensional liquid sloshing in tanks. *Journal of Computational physics*, 227(8), 3921-3939.
- [5] Celebi, M. S., Akyildiz, H. (2002). Nonlinear modeling of liquid sloshing in a moving rectangular tank. *Ocean Engineering*, 29(12), 1527-1553.
- [6] Liu, D., Lin, P. (2009). Three-dimensional liquid sloshing in a tank with baffles. *Ocean engineering*, 36(2), 202-212.
- [7] Akyildiz, H. (2012). A numerical study of the effects of the vertical baffle on liquid sloshing in two-dimensional rectangular tank. *Journal of Sound and Vibration*, 331(1), 41-52.
- [8] Chen, Y. G., Djidjeli, K., Price, W. G. (2009). Numerical simulation of liquid sloshing phenomena in partially filled containers. *Computers fluids*, 38(4), 830-842.
- [9] Navarro, H. A., Balthazar, J. M., Krasnopolskaya, T. S., Shvets, A. Y., Chavarette, F. R. (2012). Remarks on parametric surface waves in a nonlinear and non-ideally excited tank.
- [10] Balthazar, J. M., Tuset, A. M., Brasil, R. M., Felix, J. L., Rocha, R. T., Janzen, F. C., Oliveira, C. (2018). An overview on the appearance of the Sommerfeld effect and saturation phenomenon in non-ideal vibrating systems (NIS) in macro and MEMS scales. *Nonlinear Dynamics*, 93, 19-40.
- [11] Ganiev, R. F., Krasnopolskaya, T. S. (2018). The scientific heritage of VO Kononenko: the Sommerfeld–Kononenko effect. *Journal of Machinery Manufacture and Reliability*, 47, 389-398.
- [12] Dingwell, J. B. (2006). Lyapunov exponents. *Wiley encyclopedia of biomedical engineering*.
- [13] Sandri, M. (1996). Numerical calculation of Lyapunov exponents. *Mathematica Journal*, 6(3), 78-84.
- [14] Godderidge, B., Turnock, S., Tan, M., Earl, C. (2009). An investigation of multiphase CFD modelling of a lateral sloshing tank. *Computers Fluids*, 38(2), 183-193.
- [15] Sanapala, V. S., Velusamy, K., Patnaik, B. S. V. (2016). CFD simulations on the dynamics of liquid sloshing and its control in a storage tank for spent fuel applications. *Annals of Nuclear Energy*, 94, 494-509.
- [16] Singal, V., Bajaj, J., Awalgaonkar, N., Tibdewal, S. (2014). CFD analysis of a kerosene fuel tank to reduce liquid sloshing. *Procedia Engineering*, 69, 1365-1371.
- [17] Kartuzova, O. V., Kassemi, M., Hauser, D. M. (2024). Validation of a Two-Phase CFD Model for Predicting Propellant Tank Pressurization and Pressure Collapse in The Ground-Based K-Site Hydrogen SLOSH Experiment. In *AIAA SCITECH 2024 Forum* (p. 0547).
- [18] Cao, Z., Xue, M. A., Xu, G., Yuan, X., Ye, Z., Li, L., Zhang, J. (2024). Experimental and numerical study on effects of different excitations and liquid levels on sloshing in a large-scale LNG tank. *Ocean Engineering*, 308, 118343.
- [19] Young, L. S. (2013). Mathematical theory of Lyapunov exponents. *Journal of Physics A: Mathematical and Theoretical*, 46(25), 254001.
- [20] Zou, Y., Thiel, M., Romano, M. C., Kurths, J., Bi, Q. (2006). Shrimp structure and associated dynamics in parametrically excited oscillators. *International Journal of Bifurcation and Chaos*, 16(12), 3567-3579.
- [21] Stoop, R., Martignoli, S., Benner, P., Stoop, R. L., Uwate, Y. (2012). Shrimps: Occurrence, scaling and relevance. *International Journal of Bifurcation and Chaos*, 22(10), 1230032.
- [22] Lenz, W. B., Ribeiro, M. A., Tuset, A. M., Balthazar, J. M., Jarzebowska, E. (2021). Slosh Analyzes a Full Vehicle-Tank Model with SDRE Control with a Hydraulic Damper. In *Perspectives in Dynamical Systems III: Control and Stability: DSTA, Łódź, Poland December 2–5, 2019 15* (pp. 83-93). Springer International Publishing.

[23] T. S. KRASNOPOL'SKAYA AND A. Y. SHVETS, Energy Transfer Between Hydrodynamical Systems and Excitation Machines of Limited Power Supply, Proc. ENOC -St. Petersburg, Russia, June 30–July 4 , 2008.

[24] A. M. TUSSET, BALTHAZAR J. M.; BASSINELO, D. ; PONTES B.R. ; FELIX J. L. P. Statements on chaos control designs, including a fractional order dynamical system, applied to a MEMS comb-drive actuator. *Nonlinear Dynamics*, v. 69, p. 1837-1857, 2012. <https://doi.org/10.1007/s11071-012-0390-6>